Octacalcium Phosphate. 3. Infrared and Raman Vibrational Spectra

Bruce O. Fowler,*[1a] Milenko Marković,[1b,c] and Walter E. Brown[1b,d]

National Institute of Dental Research, NIH, Bone Research Branch Research Program, National Institute of Standards and Technology, Gaithersburg, Maryland 20899, and American Dental Association Health Foundation, Paffenbarger Research Center, National Institute of Standards and Technology, Gaithersburg, Maryland 20899

Received March 18, 1993. Revised Manuscript Received July 30, 1993®

Infrared and Raman band assignments are given for powdered samples of the biologically important compound, octacalcium phosphate, in the 4000–300-cm^{-1} range. Specific assignments were made for bands of the two crystallographically independent acidic phosphate groups. The numbers of observed bands were markedly less than those predicted by factor group analysis; additional unresolved bands are probably present. Infrared spectra indicate that two polymorphs of octacalcium phosphate may exist whose structures differ mainly in acidic phosphate and water bonding and in possibly different contents of water. Polymorphic forms of octacalcium phosphate are structurally plausible because of possible differences in bonding of its acidic phosphate groups and water molecules and in number of water molecules. The wavenumber positions of Raman bands, especially acidic phosphate bands, were sensitive to laser excitation power.

Introduction

A knowledge of the vibrational origin of all infrared (IR) and Raman bands of the biologically important compound octacalcium phosphate (OCP), $Ca_8(HPO_4)_2(PO_4)_4{\cdot}5H_2O$, was needed to effectively utilize both spectra to establish details of OCP structurally modified by incorporation of foreign ions and by hydrolysis. Consequently, previous IR and Raman assignments of OCP were reevaluated; several reassignments were made for IR bands, and numerous new assignments and reassignments were made for Raman bands. Specific assignments were made for bands of the two crystallographically independent HPO_4 groups in OCP; these groups can be preferentially replaced by foreign anions.

These spectral assignments were utilized in part 2[2] of this series to determine compositional and structural details of the octacalcium phosphate carboxylates (OCPCs). Since the OCPCs derive from OCP and have lattice regions similar to those in the OCP structure, detailed comparisons between OCP and OCPC spectra were used both to study the OCPCs and to facilitate and to cross-check various OCP band assignments.

This IR investigation revealed that two polymorphs of OCP (referred to in this paper as OCP(A) and OCP(B)) may exist. Thus far, however, the OCP(B) form has been observed by IR only after conversion of the OCP(A) form to the OCP(B) form due to interactions in matrixes used for IR recordings.

The band positions of certain Raman modes of OCP were found to vary considerably using different power levels of laser excitation; these wavenumber shifts were attributed to laser-induced heating and associated structural changes in OCP at the different temperatures.

Experimental Section[20]

Preparation of OCP. OCP was prepared by one of the methods of LeGeros[3] with minor modifications by Tomazic et al.[4] This OCP preparation (supplied to us by B. B. Tomazic) was analyzed for Ca and PO_4 by methods described in part 2.[2] Anal. Calcd for $Ca_8(HPO_4)_2(PO_4)_4{\cdot}5H_2O$: Ca, 32.63; PO_4, 57.98; H_2O, 9.17; Ca/PO_4 molar ratio, 1.333. Found: Ca, 32.43; PO_4 57.68; H_2O, 9.69 (calcd from mass balance); Ca/PO_4, 1.332. Optical microscopy revealed birefringent acicular crystals a few micrometers wide by about 50 μm in length. The X-ray diffraction pattern (XRD), given in part 2,[2] and the IR and Raman spectra all showed a single phase of well-crystallized OCP. Two structural forms of this OCP preparation (OCP(A) and OCP(B)) are indicated by IR spectroscopy, and this is addressed in the discussion. Additional OCP samples were prepared by the above method but with modifications in the washing procedure as described here. Specifically, 25 mL of 0.09 M calcium acetate adjusted to pH 5.1 with 0.06 mL glacial acetic acid and 25 mL of 0.08 M sodium dihydrogen phosphate (pH 4.4), both at room temperature, were simultaneously added over 15–50 min to 50 mL of stirred water at 80 ± 2 °C. The supernatant (pH 4.5) was decanted and the precipitate was quickly washed with anhydrous methanol by swirling and decanting (100 mL, three times) and finally with anhydrous ether. The precipitate was dried at 22 °C. The products were identified, using XRD, IR, and Raman spectroscopy, as single phases of well-crystallized OCP. This procedure was also utilized in an attempt to prepare deuterated OCP using an, overall, D_2O/H_2O molar ratio of about 500. On the basis of IR spectra of products, only minor deuteration occurred, which indicates strong discrimination against D_2O and D^+ in the OCP nucleation and crystal growth process.

An OCP sample prepared by the procedure of Newesely[5] was progressively hydrolyzed to hydroxyapatite (HA), $Ca_{10}(PO_4)_6(OH)_2$, by boiling the OCP in water for increasing time periods. From Ca and P analyses of the hydrolyzed solids, extents of

* Abstract published in *Advance ACS Abstracts*, September 15, 1993.

(1) (a) National Institute of Dental Research, NIH. (b) American Dental Association Health Foundation, PRC. (c) On leave of absence from the Rudjer Bošković Institute and the Faculty of Science, University of Zagreb, Zagreb, Croatia. (d) Deceased.

(2) Marković, M.; Fowler, B. O.; Brown, W. E. *Chem. Mater.*, second of three papers in this issue.

(3) LeGeros, R. Z. *Calcif. Tissue Int.* **1985**, *37*, 194.

(4) Tomazic, B. B.; Tung, M. S.; Gregory, T. M.; Brown, W. E. *Scanning Microsc.* **1989**, *3*(1), 119.

(5) Newesely, H. *Monatsh. Chem.* **1960**, *91*, 1020.

0897-4756/93/2805-1417$04.00/0

hydrolysis of OCP (Ca/P = 1.33) to HA (Ca/P = 1.67) of 34, 48, and 74% were calculated.

Infrared Spectra. IR spectra from 4000 to 300 cm^{-1} of OCP suspended in KBr pellets or slurred in fluorolube and Nujol oils were recorded at 48 °C (temperature in instrument light beam) using a Perkin-Elmer Model 621 spectrophotometer purged with dry CO_2-free air.

KBr pellets were prepared by mixing (not grinding) the preground OCP (0.5 to 1.5 mg, particle size <5 μm) with 400 mg of IR-quality KBr (about 20–40-μm particle size) in a steel capsule on a mechanical shaker and then pressing the mixture in a 13-mm diameter evacuated die under a total force of 53 380 N (12 000 pound force) for 30 s. Grinding the sample and KBr together was avoided to reduce additional moisture adsorption from the ground and smaller KBr particle size. KBr sample pellets were run versus a blank KBr pellet in the reference beam to cancel KBr impurity bands, mainly H_2O bands.

Fluorolube and Nujol mulls containing about 5-μm particle size OCP supported between thallium bromide–iodide plates were used for recordings in the 4000–1310- and 1320–300-cm^{-1} ranges, respectively, with sample concentrations adjusted to be the same in the two ranges.

The wavenumber accuracy, calibrated against standard indene bands,[6] was ±1 cm^{-1} for sharp bands and several cm^{-1} for broad bands. Spectral slit widths were about 6 cm^{-1} above 2000 cm^{-1} and 3–5 cm^{-1} below 2000 cm^{-1}.

Raman Spectra. Raman spectra were recorded with a Spex Model 1401 spectrometer in the 4000–300-cm^{-1} region using 488.0- and 514.5-nm wavelength excitation from an argon ion laser. Spectra were obtained from (a) about 5 mg of the sample powder pressed into a 3-mm-diameter pellet in a die under a force of 445–1110 N (100–250 pound force) for 5 min and (b) from about 4 mg of sample powder, and lesser amounts (<0.5 mg) for smaller wells, that was tamped in a cylindrical well (2.5-mm diameter, 1 mm deep) in the center of an aluminum disk 1.5 mm thick and 13 mm in diameter followed by pressing under a sufficient force of about 71 170 N (16 000 pound force) for 5 s to reduce disk thickness, constrict sample well and compact sample. The exciting radiation was focused on the sample pellet or compacted sample in the disk tilted about 30° from the incoming beam direction that was upward and vertical; scattered radiation was collected at 90° to the incoming beam direction and detected by a RCA C31034 photomultiplier cooled to −25 °C.

Raman spectra of OCP were obtained using 488.0- and 514.5-nm wavelength excitation at power levels ranging from about 40 to 400 mW all measured at the sample. The OCP spectrum in Figure 2 was obtained using 200 mW of 488.0-nm excitation and those in Figure 5, 85 and 380 mW of 488.0 nm excitation as designated. The wavenumber positions of many OCP bands depended on excitation power. Consequently, OCP band positions measured using 488.0-nm excitation at low (50–85 mW), medium (175–200 mW), and high (350–400 mW) powers are given in Table I. These different wavenumber positions versus excitation power are expected to arise from localized sample heating and may vary considerably under slightly different irradiance and sample conditions. The degree of sample heating and the associated band wavenumber shifts depend on how well the laser light is focused and on the physical texture of the compacted powdered samples. Loosely compacted powders are expected to reach higher temperatures in the focused laser beam than well compacted powders. The OCP sample pellets were at room temperature in the spectrometer; the temperature at the focused laser impingement point (about 100-μm^2 area) on the pellet surface was not measured but was estimated to be slightly above room temperature at low power (50–85 mW) and about 80 to 100 °C at high power (350–400 mW) using 488.0-nm excitation.

Raman spectra were also obtained from compacted OCP powder in an aluminum disk at 25 and 90 °C mounted in a variable-temperature cell using 488.0-nm excitation at a power of 40 mW. The aluminum disk temperature was measured a few millimeters from the sample and not at the point of focused irradiance. Comparisons of spectra obtained at 40 mW from the pellet heated at 90 °C with spectra obtained at 380 mW from the unheated pellet in ambient surroundings were used to estimate the pellet temperature of about 90 °C using 380 mW of power.

The spectral slit widths were 5 and 3 cm^{-1}, respectively, for spectra in Figures 2 and 5. The wavenumber accuracy was ±1 cm^{-1} based on calibration using standard neon emission lines[7] from a neon lamp.

The baselines (BL) in Figures 2 and 5 were obtained by reflecting the 488.0-nm line from a piece of rough surface platinum foil placed in the normal sample position. Bands in the BL arise from "grating ghosts" and these spurious bands in OCP spectra are denoted. OCP spectra obtained from both 488.0- and 514.5-nm wavelength excitation were utilized to discern OCP bands from ghost bands.

Results and Discussion

OCP Structure and Vibrational Modes. The structure of OCP has recently been refined,[8] and a projection down the c axis is shown in Figure 1. OCP crystallizes in the triclinic system, space group $P\bar{1}$-C_i^1, with two $Ca_8(HPO_4)_2(PO_4)_4 \cdot 5H_2O$ formula units per unit cell. The four PO_4^{3-}, two HPO_4^{2-}, and five H_2O groups in the asymmetric half cell are all on C_1 symmetry sites, are all crystallographically distinct, and are related by a center of symmetry in the full unit cell. The OCP structure consists of two alternating layers parallel to (100) that are designated the apatitic layer (denoted by dotted circles) and the hydrated layer (denoted by open circles).[8] The nonequivalent groups are designated PO_4 (1–4), HPO_4 (5 and 6), and H_2O (1–5). The PO_4 (1–4) groups are structurally similar, but 1 and 4 in the apatitic layer and 2 and 3 at the junction of the apatitic and hydrated layers form more similar pairs. The HPO_4(5) group, located in the hydrated layer, and the HPO_4(6) group, located at the junction of the apatitic and hydrated layers, are each distinctly different; HPO_4(6) has a shorter and stronger intermolecular hydrogen bond than that of HPO_4(5). Of the structurally different H_2O (1–5) molecules in the hydrated layer, H_2O(3), statistically located in two sites (3a and 3b), has the shortest intermolecular hydrogen bond; H_2O(4) is located in a position similar to the OH position in HA; and H_2O(5) appears more weakly hydrogen bonded than the others.

The eight PO_4 groups in the unit cell each distorted to C_1 symmetry are predicted to give rise to 72 internal vibrations that split under the C_i factor group into 36 A_g and 36 A_u modes with each 36 mode symmetry type composed of $4\nu_1$, $8\nu_2$, $12\nu_3$, and $12\nu_4$ type PO_4 modes. The A_g and A_u modes are Raman and IR active, respectively; the ν mode numberings for the PO_4 and HPO_4 (discussed below) vibrations are those for tetrahedral groups.

The $HOPO_3$ group has 12 internal vibrational modes three of which derive from OH modes and these are separately discussed below. Considering the OH group as a single point mass, each HPO_4 group distorted to C_1 symmetry is predicted to have 9 A modes both IR and Raman active. Since two structurally different HPO_4 (5 and 6) groups are present, two sets of 9 A modes, with each set having different wavenumbers, are predicted. In addition, because the unit cell contains two HPO_4(5) groups and two HPO_4(6) groups related by a center of symmetry, the modes of each equivalent pair are predicted under the C_i factor group to split into 9 A_g + 9 A_u modes with two

(6) Jones, R. N.; Nadeau, A. *Spectrochim. Acta* **1964**, *20*, 1175.

(7) Loader, J. *Basic Laser Raman Spectroscopy*; Heyden: London, 1970; Chapter 3.

(8) Mathew, M.; Brown, W. E.; Schroeder, L. W.; Dickens, B. *Crystallogr. Spectrosc. Res.* **1988**, *18*(3), 235.

Table I. Infrared and Raman Wavenumbers (cm^{-1}) and Assignments of Octacalcium Phosphate Bands

infrared[a]			Raman[b]				
A form	B form	Δ cm^{-1} (A − B)	H	L	M	Δ cm^{-1} (H − L)	assignment
	~3600 vvw, sh						ν_3, ν_1 stretch of H-bonded H_2O, HPO_4 (OH stretch)
~3555 m, b	3525 m						
	~3300 m, b		NM[c]	NM[c]	NM[c]		
~2950 m, b	~3090 m, b						
~2400 vw, b	~2440 vw, b						HPO_4(6) (OH stretch)
1629 w	1642 w	−13	NM[d]	NM[d]	~1630 vw, b		ν_2 H_2O bend
~1298 vw	1295 w	+3					HPO_4(6) (OH in-plane bend)
1207 w	1193 w	+14					HPO_4(5) (OH in-plane bend)
1138 vw, sh	~1137 vvw, sh	+1					ν_3 HPO_4 stretch
1118 s	1121 s	−3					ν_3 HPO_4(6) stretch
1109 s	1103 s	+6	~1105 vw	~1112 w	~1109 vw	−7	ν_3 HPO_4(5) stretch
1093 s							
1086 s	1077 s	+9	1084 vw	1079 vw	1079 vw	+5	ν_3 HPO_4, ν_3 PO_4 stretch
				~1052 w	~1052 vw		
						1050[e] w	
1056 s	1055 s	+1					
			~1048 w	1048 w			ν_3 PO_4 stretch
1038 s	1037 s	+1	1036 w	~1036 vw	1036 vw		
1023 s	1023 s	0	~1025 vw	~1027 vw	~1025 vw		
	~1000 vvw, sh		1008 m	1011 m	1010 m	−3	ν_1 HPO_4 stretch
				~1005 w, sh	~1005 w, sh		
967 w			967 vs	966 s	966 s	+1	ν_1 PO_4 stretch
963 w	962 w	+1	956 vs	959 vs	957 vs	−3	
913 w	917 w	−4	913 w	916 w	916 w	−3	HPO_4(6) [P−(OH)] stretch
873 w	861 w	+12	884 w	874 w	879 w	+10	HPO_4(5) [P−(OH)] stretch
~650 vw, b			~630 vw	~631 vw	~630 vw		H_2O libration
627 vw	627 vw	0					H_2O(4) libration
608 vvw, sh			617 vw, sh	619 vw, sh	618 vw, sh	−2	ν_4 PO_4 bend
599 m	601 m	−2	606 mw	609 mw	609 mw	−3	
578 w	575 w	+3	588 m	591 m	591 m	−3	ν_4 PO_4, ν_4 HPO_4 bend
			578 m	577 m	578 m	+1	
561 m	560 m	+1					ν_4 PO_4 bend
			~556 vw, b		~556 vw, b		ν_4 HPO_4 bend
529 w	524 w	+5	533 w, b	523 w, b	527 w, b	+10	
465 vw	466 vw	−1	449 m	451 m	450 m	−2	ν_2 PO_4 bend
			426 m	427 m	426 m	−1	
445 vw	449 vw	−4					H_2O libration
			~413 m, sh	409 m	413 m, sh	+4	ν_2 HPO_4 bend
			371 w	353 w	356 w	+18	ν_2 HPO_4(5) bend
	360 w						
337 m	~345 w	~−15[f]					Ca−H_2O translation

[a] Infrared band positions for A and B forms at 48 °C and wavenumber differences between forms (A − B). [b] Raman band positions for excitation with 488.0-nm radiation at low (L), medium (M), and high (H) power levels (L = 50–85 mW; M = 175–200 mW; H = 350–400 mW) and wavenumber differences between excitation at high and low powers (H − L) where discernible. [c] The spectrum has a broad unresolved water band that extends from about 3700 to about 2000 cm^{-1}. [d] Very broad weak band. [e] Center of 1048 and 1052 cm^{-1} doublet. [f] From average of 360- and 345-cm^{-1} bands. NM = not measured, w = weak, mw = medium to weak, m = medium, s = strong, v = very, sh = shoulder, b = broad.

resultant sets of (9 A_g + 9 A_u) modes having different wavenumbers comprised of ($2\nu_1$, $4\nu_2$, $6\nu_3$, $6\nu_4$) A_g modes and ($2\nu_1$, $4\nu_2$, $6\nu_3$, $6\nu_4$) A_u modes. Each $HOPO_3$ group has one OH stretching and two OH bending modes (an in-plane and an out-of-plane mode); all three are both IR and Raman active. The wavenumber of these three modes for the nonequivalent HPO_4 (5 and 6) groups are expected to be different and a center of symmetry between the equivalent $HOPO_3$ pairs is predicted to split modes of each set into A_g and A_u modes.

The 30 internal modes of the 10 H_2O groups distorted to C_1 symmetry are predicted under the C_i factor group to split into 15 A_g and 15 A_u modes with each symmetry type composed of $5\nu_1$, $5\nu_2$, and $5\nu_3$ type H_2O modes.

Spectral bands arising from external or lattice modes (translations and rotations) are, overall, not considered here. The calcium and phosphate translational and phosphate rotational modes are expected to occur below about 350 cm^{-1} by comparison with those of HA;[9] this lower wavenumber region was not studied here. External modes of the H_2O groups, however, and especially rotational type modes of hydrogen-bonded H_2O groups,[10] may have wavenumbers as high as 850 cm^{-1}, and bands for these modes are expected in OCP spectra.

Infrared and Raman Spectra of OCP. IR and Raman spectra of OCP in the 4000–300-cm^{-1} range are shown in Figure 2, and the band wavenumbers and assignments are given in Table I. The principal differences between IR spectra of the OCP A and B forms above 2000 cm^{-1} are differences in band positions and relative intensities and below 2000 cm^{-1}, shifts in positions of corresponding bands of each form. The IR wavenumber positions of the OCP-(B) form bands are used in the following assignment section and bands of both forms are discussed in a later section. Similarly, the Raman wavenumbers of OCP bands obtained under medium (M) excitation power (Table I) are used in the following band assignment section and shifted band positions, observed at higher (H) and lower (L) power, are discussed later.

(9) Fowler, B. O. *Inorg. Chem.* **1974**, *13*, 194.

(10) (a) Petrov, I.; Soptrajanov, B.; Fuson, N.; Lawson, J. R. *Spectrochim. Acta* **1967**, *23A*, 2637. (b) Raghuvanshi, G. S.; Khandelwal, D. P.; Bist, H. D. *Appl. Spectrosc.* **1984**, *38*(5), 710.

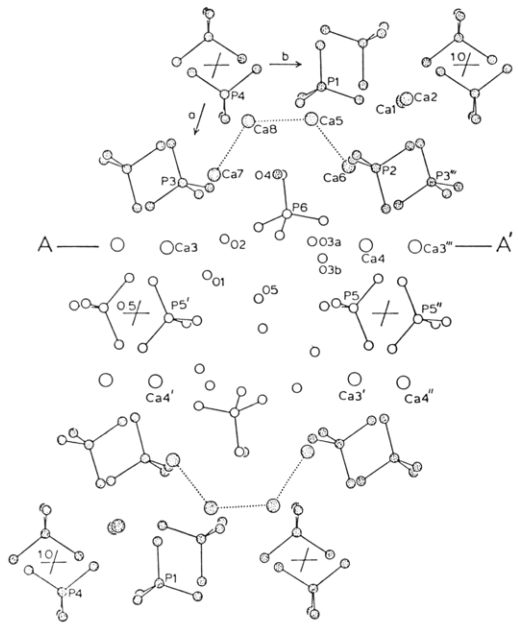

Figure 1. Structure of octacalcium phosphate projected down the *c* axis. The unfilled circles denoted (O1, O2, O3a, O3b, O5) and dotted circle O4 are water molecules; hydrogen atoms are not shown. After ref 19.

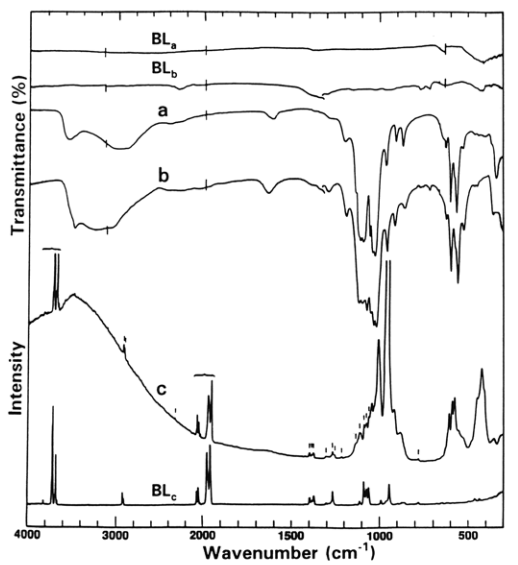

Figure 2. Infrared transmittance spectra (a, b) and Raman spectrum (c) of octacalcium phosphate (OCP) from 4000 to 300 cm^{-1}. Spectrum (a) shows the OCP(A) form recorded from a KBr pellet and (b) the OCP(B) form recorded from an oil mull. BL_a denotes the KBr pellet baseline and BL_b the oil mull baseline. Braces and short vertical lines above the Raman spectrum (c) denote spurious bands arising from its baseline (BL_c); the broad ascending Raman intensity from about 1500 to 4000 cm^{-1} originated from fluorescence from the laser-irradiated OCP sample.

band positions, observed at higher (H) and lower (L) power, are discussed later.

The IR and Raman band assignments given in Table I are based on (1) factor group analysis, (2) comparisons with previously assigned PO_4, HPO_4, and H_2O modes of OCP (IR[11,12] Raman[13]) and related compounds, HA (IR[9,14a] Raman[15]), $CaHPO_4$ (IR[14b] Raman[16]) and $CaHPO_4 \cdot 2H_2O$ (IR[14b,17] Raman[17]), (3) band position and intensity correspondence between IR and Raman bands, and (4) IR and Raman band changes on progressive hydrolysis of OCP to HA and on incorporation of dicarboxylate groups for HPO_4 groups in the OCP structure (part 2[2]). As already noted, our preliminary attempts to prepare deuterated OCP, to facilitate more definitive assignments of certain bands, were unsuccessful.

The IR assignments in Table I for OCP(B) overall agree with previous assignments, but several reassignments and specific designations for bands of the structurally different HPO_4 (5 and 6) groups are made here. A literature search indicated that no detailed Raman band assignments have been reported for OCP. The Raman band positions of OCP in the 1110–240-cm^{-1} range have been reported[13] and are overall close to band positions given in Table I. In this previous report,[13] however, the Raman bands were discussed only in terms of PO_4 vibrations, and no assignments were made for HPO_4 vibrations; reassignments of many of the PO_4 vibrations to HPO_4 vibrations are given here.

The main argument for designating specific HPO_4 bands to either HPO_4 (5 or 6) is as follows. When OCP is hydrolyzed to HA, a preferential decrease in $HPO_4(6)$ relative to $HPO_4(5)$ is expected because of their sites in OCP (Figure 1): to initially form the PO_4 and Ca triads in the HA structure, $HPO_4(6)$ must be removed or displaced whereas less significant changes in $HPO_4(5)$, located in the water layer, are expected.

IR spectra in the 1400–700- and 3700–3400-cm^{-1} ranges of OCP progressively hydrolyzed (34, 48, and 74%) to HA are shown in Figure 3. The intensity of the OH stretching band of HA (3572 cm^{-1}) progressively increased with increased hydrolysis. The intensities of bands at 861 and 1193 cm^{-1} did not change substantially on hydrolysis (except broadening and a higher wavenumber shift of the 1193 cm^{-1} band); these bands are, respectively, assigned to P–(OH) stretch and OH in-plane bend of $HPO_4(5)$. The intensities of the bands at 917 and 1295 cm^{-1} preferentially decrease, compared to the 861- and 1193-cm^{-1} bands, on hydrolysis; consequently, the 917- and 1295-cm^{-1} bands are, respectively, assigned to P–(OH) stretch and OH in-plane bend of $HPO_4(6)$. Raman spectra (not shown) of the progressively hydrolyzed OCP samples also showed a preferential intensity decrease of the 916-cm^{-1} band relative to the 879-cm^{-1} band; the Raman 916- and 879-cm^{-1} bands are assigned to P–(OH) stretch of $HPO_4(6)$ and $HPO_4(5)$, respectively. The OH in-plane bending bands of hydrogen-bonded HPO_4 groups have very weak Raman intensity[16,17] and they were not detected in the about 1350–1150-cm^{-1} region.

The assignments and reassignments are as follows:

(1) The IR band at 917 cm^{-1} previously assigned[12] to an OH out-of-plane bending mode of one of the HPO_4 groups is reassigned to P–(OH) stretch of $HPO_4(6)$ based on the

(11) Fowler, B. O.; Moreno, E. C.; Brown, W. E. *Arch. Oral Biol.* **1966**, *11*, 477.
(12) Berry, E. E.; Baddiel, C. B. *Spectrochim. Acta* **1967**, *23A*, 1781.
(13) Nelson, D. G. A.; Williamson, B. E. *Caries Res.* **1985**, *19*, 113.
(14) (a) Ross, S. D. In *The Infrared Spectra of Minerals*; Farmer, V. C., Ed.; Mineralogical Society: London, 1974; Chapter 17, p 390 and references therein (note the ν_2 PO_4 mode has been assigned to higher wavenumbers; see ref 9); (b) p 393.
(15) (a) Griffith, W. P. *J. Chem. Soc.* (*A*), **1970**, 132. (b) Blakeslee, K. C.; Condrate, R. A., Sr. *J. Am. Ceram. Soc.* **1971**, *54*, 559. (c) O'Shea, D. C.; Bartlett, M. L.; Young, R. A. *Arch. Oral Biol.* **1974**, *19*, 995. (d) Fowler, B. O. *J. Dent. Res.* **1977**, *56* (Special Issue B), Abstract No 68. (e) Iqbal, Z.; Tomaselli, V. P.; Fahrenfeld, O.; Möller, K. D.; Ruszala, F. A.; Kostiner, E. *J. Phys. Chem. Solids* **1977**, *38*, 923. (f) Nelson, D. G. A.; Williamson, B. E. *Aust. J. Chem.* **1982**, *35*, 715.
(16) Casciani, F.; Condrate, R. A., Sr. *J. Solid State Chem.* **1980**, *34*, 385.
(17) Casciani, F.; Condrate, R. A., Sr. *Spectrosc. Lett.* **1979**, *12*, 699.

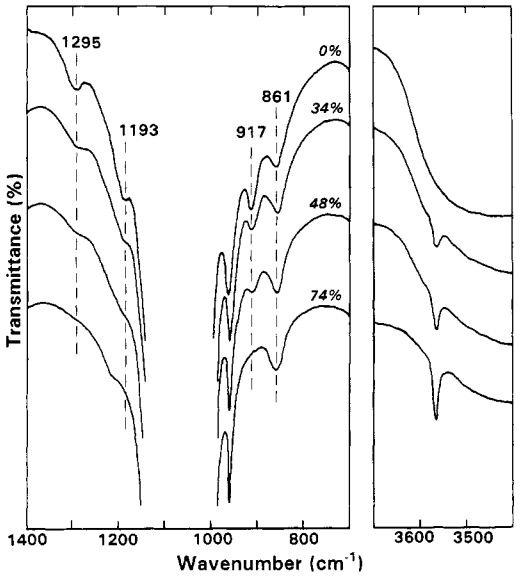

Figure 3. Infrared spectra recorded from KBr pellets of octacalcium phosphate (OCP) samples that were progressively hydrolyzed in solution to hydroxyapatite (HA) in the 1400–700 cm^{-1} and 3700–3400-cm^{-1} regions. The extents of hydrolysis of OCP to HA are denoted by 0, 34, 48, and 74%.

following. Its corresponding Raman band at 916 cm^{-1} has an intensity similar to that of the 879-cm^{-1} Raman band assigned here to P–(OH) stretch of $HPO_4(5)$; if the 916-cm^{-1} Raman band derived from OH out-of-plane bend, rather than P–(OH) stretch, a much weaker band intensity would be expected. Thus, the Raman data indicate the corresponding IR band at 917 cm^{-1} also arises from P–(OH) stretch. During progressive hydrolysis of OCP to HA, the 917-cm^{-1} IR band and the 916-cm^{-1} Raman band both assigned to $HPO_4(6)$ both decrease in intensity more rapidly than the IR band at 861 cm^{-1} and its corresponding Raman band at 879 cm^{-1}, both assigned to $HPO_4(5)$.

(2) Similarly, the IR bands at 1295 and 1193 cm^{-1} are assigned to $HPO_4(6)$ and $HPO_4(5)$, respectively, because of the preferential decrease in the 1295-cm^{-1} band intensity on progressive hydrolysis of OCP to HA. Moreover, HPO_4-(6) has a shorter and stronger intermolecular hydrogen bond than $HPO_4(5)$; thus, its OH in-plane bending mode is expected at higher wavenumbers than that of $HPO_4(5)$ which is consistent with the above assignments. This is in accord with previous IR interpretation of two differently hydrogen-bonded HPO_4 groups but without specific designation to HPO_4 (5 or 6).[12]

(3) The IR ν_3 HPO_4 stretching bands at 1121 and 1103 cm^{-1} appear to arise from $HPO_4(6)$ and $HPO_4(5)$, respectively, and the Raman bands at 1109 and 356 cm^{-1} from ν_3 $HPO_4(5)$ stretch and ν_2 $HPO_4(5)$ bend, respectively. These IR and Raman band designations to either HPO_4 (5 or 6) groups are based on HPO_4 band intensity changes observed in part 2[2] for OCP having its $HPO_4(5)$ groups replaced by dicarboxylate groups.

(4) The IR 1077-cm^{-1} band[12] and the 575-cm^{-1} band[11,12] were previously assigned to PO_4 modes only. Detailed spectral comparison, however, of PO_4 and HPO_4 salts showed bands of both groups occur near these wavenumbers; thus, both groups are listed for these wavenumbers in Table I.

(5) The IR ν_2 PO_4 modes, previously assigned to lower wavenumber bands at 350[11,12] and 275[12] cm^{-1}, are reassigned to the band(s) at 466 cm^{-1} by comparison to ν_2 PO_4 assignments for HA.[9] The weak IR band at 449 cm^{-1} could be a second component of ν_2 PO_4, but its reported shift on deuteration identifies it as a H_2O librational band.[12]

(6) The IR ν_2 HPO_4 components, previously assigned[12] to bands at 335 and 262 cm^{-1}, are expected to occur at higher wavenumbers, about 440 to 390 cm^{-1}, by comparison to IR ν_2 HPO_4 band assignments for several other HPO_4 containing compounds.[10a,14b,17] The weak intensity ν_2 HPO_4 IR components, expected in the 440–390 cm^{-1} region, were not detected. The IR bands at 360 and about 345 cm^{-1} are reassigned to external modes and probably arise from Ca–H_2O translations. The Raman ν_2 HPO_4 bands, expected to have higher intensities than those of the corresponding undetected IR bands, are assigned to the medium intensity shoulder at 413 cm^{-1} and the weak band at 356 cm^{-1}. The 356-cm^{-1} band is essentially missing when $HPO_4(5)$ groups are replaced by dicarboxylate groups (part 2[2]); thus, this band is assigned to the $HPO_4(5)$. This 356-cm^{-1} band is about 25–35 cm^{-1} lower in position than the corresponding ν_2 HPO_4 components of $CaHPO_4 \cdot 2H_2O$ and $CaHPO_4$ which causes some uncertainty in this assignment. However, at higher laser excitation powers (Table I), the 356-cm^{-1} band and several of the other HPO_4 bands shift considerably to higher wavenumbers; these correlative shifts support assignment of the 356-cm^{-1} band to a HPO_4 mode.

(7) The very weak IR band near 627 cm^{-1} was previously assigned to libration of $H_2O(4)$[12] or to OH libration from a HA impurity[11] phase in OCP. This $H_2O(4)$ molecule is located at the junction of the apatitic and water layers in OCP (Figure 1) and adjacent to $HPO_4(6)$ and possibly hydrogen bonded to it.[8] Since spectra in part 2[2] show dicarboxylate anion incorporations effect only minor structural changes in PO_4 groups in the OCP apatitic layer and in $HPO_4(6)$, the structurally adjacent $H_2O(4)$ molecule is also not expected to be significantly changed. Thus, the persistence and nearly constant intensity of the about 627 cm^{-1} band in IR spectra of the OCPCs (part 2[2]) along with lack of a substantial HA impurity phase (3572-cm^{-1} IR OH band for HA was not detected) support assignment to the $H_2O(4)$ molecule. Previous IR assignments for OCP $H_2O(4)$ stretching bands were at 3581 and 3561 cm^{-1} (at −180 °C).[12] However, since the IR 3525-cm^{-1} OCP band (Table I) also persists in OCPC spectra (part 2[2]), this band appears a better choice for the $H_2O(4)$ stretching assignment.

Differences in relative intensities of corresponding IR and Raman bands, assigned in Table I and shown in Figure 2, are consistent with assignments and expectations. The ν_1 and ν_2 PO_4 and ν_1 HPO_4 Raman band intensities are strong, whereas intensities of the corresponding IR bands are weak; the IR ν_3 PO_4 band intensities are strong, whereas the corresponding Raman band intensities are weak. The numbers of observed bands are markedly less than those predicted; many more unresolved bands are probably present.

Infrared Spectra of OCP Polymorphs. This IR study revealed that two polymorphs of OCP, here designated OCP(A) and OCP(B), may exist. Their spectral differences are obvious (Figures 2 and 4, and Table I). Thus far, only the OCP(A) form has been detected by IR for different OCP samples; the OCP(B) form has not been initially detected for OCP samples but only after suspension and interaction in matrixes used for IR recording as described below. OCP(A) spectra were observed for particles

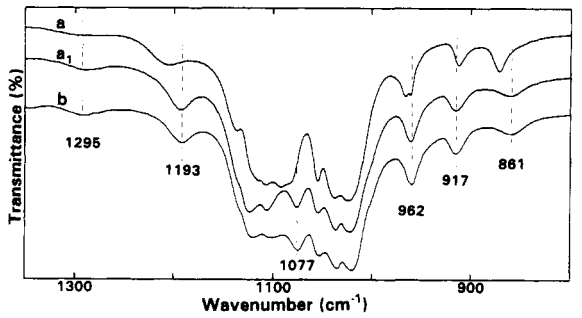

Figure 4. Infrared spectra of octacalcium phosphate (OCP) from 1350 to 800 cm^{-1}. Spectrum (a) shows the OCP(A) form recorded from a KBr pellet about 1 h after pellet preparation and spectrum (a_1) is after the OCP(A) form in the KBr pellet has aged (see text) and converted to the OCP(B) form. Spectrum (b) is from an about 1-h old Nujol mull of the same OCP used for the pellet spectrum (a) above that has converted in the mull to the OCP(B) form. The dashed lines designate band positions for the OCP-(B) form, spectra a_1 and b.

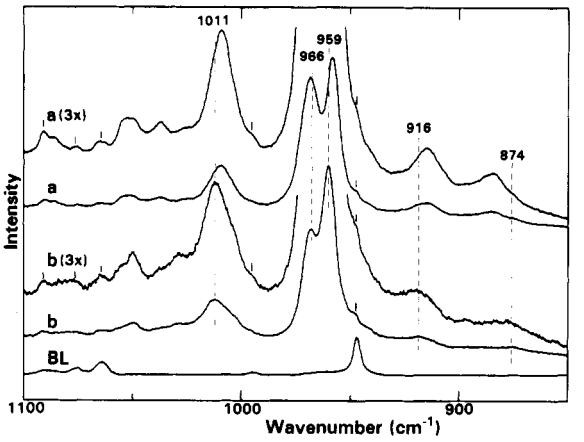

Figure 5. Raman spectra of octacalcium phosphate obtained using 488.0-nm wavelength excitation at different powers, 380 mW (a and intensity expanded three times, a (3×)) and 85 mW (b, b (3×)), from 1100 to 850 cm^{-1}. The dashed lines designate band positions in (b, b (3×)) spectra. The short vertical lines above spectra denote spurious bands arising from their baseline (BL).

suspended in or supported on different matrixes (dry KBr pellets or polyethylene films) whereas OCP(B) spectra were observed for the same particles only in damp KBr pellets or in oil mulls between Tl(Br,I) or KBr plates. IR spectra of OCP from a freshly prepared (about 30 min age) dry KBr pellet (unground original KBr powder) always showed OCP(A) whereas spectra of the same OCP from a damp KBr pellet (KBr powder ground and exposed to laboratory atmosphere for 30 min at 55% relative humidity) showed the OCP(B) form. Conversion from OCP-(A) to OCP(B) was reversible in the same KBr pellet depending on its moisture content: OCP(A) in dry KBr converted to OCP(B) in <1.6 days at 48 °C and 55% relative humidity; this OCP(B) converted to OCP(A) in <19 days at 22 °C and 0% relative humidity; this OCP(A) converted to OCP(B) in <1 day at 22 °C and 55% relative humidity. This reversibility excludes pressure, required to form the pellet, and differences in indexes of refraction of different matrixes as sources causing the spectral differences observed for the two forms. Spectra of all fluorolube and Nujol mulls of OCP between KBr or Tl-(Br,I) plates showed OCP(B) regardless of mull age (about 1 h to several days); the same OCP run as Nujol mulls or powders only on polyethylene films showed OCP(A). The combined dry OCP(A) and damp OCP(B) KBr pellet spectral data and the polyethylene film OCP(A) spectral data show that both water and the ionic KBr matrix are necessary for the conversion. Three OCP samples prepared at 80 °C and one at 22 °C were all OCP(A) from spectra of the powders in dry KBr pellets. Further IR examination of differently prepared OCPs having possibly different structural forms may detect OCP(B) in dry KBr pellets and independent of matrix interactions, observed thus far, to form it.

The IR spectra (Figures 2 and 4) and relative differences in wavenumber positions (Table I) or OCP(A) and OCP-(B) bands show considerable differences in H_2O and HPO_4 bonding and minor differences in PO_4 bonding; this establishes that the principal structural differences between the two forms are in the hydrated layer of OCP. As compared to OCP(B), OCP(A) has a more strongly hydrogen-bonded water component (about 2950-cm^{-1} band) and also a more strongly hydrogen-bonded HPO_4-(5) group based on its higher OH in-plane bend at 1207 cm^{-1} (1193 cm^{-1} for OCP(B)). The HPO_4(6) groups at the junction of the apatitic and hydrated layers are only slightly different in the two forms based on their minor wavenumber differences of about 4 cm^{-1}.

Polymorphic forms of OCP are plausible because of possible differences in hydrogen-bond arrangements of the 4 HPO_4 groups and 10 H_2O molecules in the hydrated layer of the OCP unit cell. Different arrangements of the HPO_4 groups, water molecules, and a different degree of hydration, 9 or 11 H_2O, could change the OCP space group from $P\bar{1}$ to $P1$. The OCP(A) and OCP(B) forms observed in dry and damp KBr pellets, respectively, suggest that the degree of hydration is an important factor.

Effect of Temperature on Raman Band Positions. The positions of Raman bands of OCP varied about −3 to +18 cm^{-1} depending on laser power used to obtain spectra (Table I and Figure 5). These different band positions obtained at 86 and 380 mW were completely reversible by changing laser power at the irradiated point on the OCP pellet provided that the higher power used did not decompose the OCP. Laser powers above about 400 mW usually resulted in decomposition of the OCP, but this was variable depending on a combination of factors including focus of the laser beam, physical texture of the OCP pellet (loosely versus well compacted particles), and resultant heat transfer from the pellet. Raman spectra obtained at a constant low laser power of 40 mW from a well-compacted OCP pellet progressively heated in a variable-temperature cell from 25 to 90 °C showed essentially the same band intensity changes and positions at 90 °C as were observed for the unheated pellet irradiated at higher power of 380 mW; this indicates a sample temperature of about 90 °C using a laser power of 380 mW. The variable-laser-power data obtained on the compacted pellets of OCP demonstrate the Raman band shifts and intensity changes that can be expected for pellet temperatures between about room temperature and 90 °C. Raman spectra of loosely compacted powders are expected to show the same band shifts but at lower laser power levels because of poor heat transfer and higher sample temperatures. These wavenumber shifts versus increasing laser power are attributed to heating and resultant lattice expansion and structural differences in OCP at the different induced temperatures. On heating from room temperature to 90 °C, and PO_4 bands overall

shifted about 1–3 cm^{-1} to lower wavenumbers but the second ν_1 PO_4 component at 966 cm^{-1} increased in intensity and shifted to 967 cm^{-1}. These shifts to lower wavenumbers are expected for vibrational modes which experience decreased repulsive forces effected by increased intermolecular distances concomitant with lattice expansion on heating.[18] The P–(OH) stretching band of the HPO_4(6) group (located at the junction of the apatitic and hydrated layers) shifted 3 cm^{-1} to lower wavenumbers on heating to 90 °C (similar to most PO_4 band shifts) whereas the P–(OH) stretching band of the HPO_4(5) group (located in the hydrated layer) shifted 10 cm^{-1} to higher wavenumbers and its ν_2 bending band shifted 18 cm^{-1} to higher wavenumbers. These larger HPO_4(5) band shifts, and also their directions to higher wavenumbers on heating, indicate a considerable difference in bonding at 90 °C of HPO_4(5) compared to the HPO_4(6) and PO_4 groups. At 90 °C some of the 10 H_2O molecules in the hydrated layer may be differently hydrogen bonded to each other and in turn alter the hydrogen bonds between HPO_4(5) and H_2O molecules (HOH- - -OO_2POH- - -OH_2).

Coincidence of Spectral Bands. A comparison of wavenumbers of corresponding IR and Raman bands for noncoincidence was not straightforward because of the two different sets of IR wavenumbers for the OCP(A) and OCP(B) forms, lack of an OCP(B) form for Raman spectra, and differences in Raman band positions observed for different laser excitation powers. The OCP pressed into a pellet and used for Raman spectra is expected to be the OCP(A) form and the OCP pellet temperature at the lower laser power is expected to be closer to the IR KBr pellet temperature of about 48 °C. Consequently, the comparison with least uncertainty appears to be between wavenumbers of the IR OCP(A) form and Raman OCP wavenumbers obtained at low laser power. Using these for comparison, the PO_4 wavenumber positions of the IR OCP(A) form bands and the Raman OCP bands observed at low laser power are, overall, noncoincident and especially for the ν_4 and ν_2 PO_4 bands (differences in band positions of $\geq$3 cm^{-1} were considered noncoincident). This overall noncoincidence of IR and Raman PO_4 band positions is in accord with the OCP(A) form having a center of symmetry with respect to the 8 PO_4 ions in the unit cell.

Considering the HPO_4 ions as separate sublattices in the OCP structure, it is uncertain from the spectral data if the set of two HPO_4(5) ions and the set of two HPO_4(6) ions each have a local center of symmetry. This is because of the limited number of bands available for comparison and to wavenumber uncertainty because of broadness of some of the HPO_4 bands. Nonetheless, the HPO_4(5) set has IR bands at 873 and 1109 cm^{-1} and Raman bands at about 874 and about 1112 cm^{-1}; this near coincidence suggests that the two HPO_4(5) ions in the OCP(A) form may not have a local center of symmetry. Similarly, the HPO_4(6) set has IR and Raman bands at 913 and 916 cm^{-1}, respectively, this slight noncoincidence suggests a center of symmetry may be present for this pair in the OCP(A) form. The IR and Raman bands at 529 and about 523 cm^{-1}, respectively, derive from ν_4 HPO_4 modes but without specific designation to the HPO_4 (5 or 6) groups. Since the expected separate ν_4 bands from the different HPO_4 (5 and 6) groups were not resolved and identified, a coincidence comparison of these bands is ambiguous.

Acknowledgment. We especially thank M. Mathew, ADAHF, PRC, NIST, for advice and helpful discussions on the structure of OCP. This work was supported by (a) USPHS Research Grant DE-05030 to the American Dental Association Health Foundation by the National Institutes of Health and is part of the dental research program conducted by NIST in cooperation with ADAHF, and by (b) the Ministry of Science, Technology and Informatics of Croatia. M.M. gratefully acknowledges financial support from the Fulbright Scholarship Exchange Program.

(18) (a) Schroeder, R. A.; Weir, C. E.; Lippincott, E. R. *J. Res. Nat. Bur. Stand., Sect. A.* **1962**, *66*, 407. (b) Fowler, B. O. *Inorg. Chem.* **1974**, *13*, 207.

(19) Mathew, M.; Brown, W. E. *Bull. Chem. Soc. Jpn.* **1987**, *60*, 1141.

(20) Certain commercial materials and equipment are identified in this paper to specify the experimental procedure. In no instance does such identification imply recommendation or endorsement by the National Institute of Standards and Technology, the National Institutes of Health, or the ADA Health Foundation or that the material or equipment identified is necessarily the best available for the purpose.